arXiv:cond-mat/0406226v1 [cond-mat.str-el] 9 Jun 2004

Tuning the magnetism of ordered and disordered strongly-correlated electron nanoclusters

Nicholas Kioussis, Yan Luo, and Claudio Verdozzi*
Department of Physics, California State University Northridge, California 91330-8268

Recently, there has been a resurgence of intense experimental and theoretical interest on the Kondo physics of nanoscopic and mesoscopic systems due to the possibility of making experiments in extremely small samples. We have carried out exact diagonalization calculations to study the effect of energy spacing Δ in the conduction band states, hybridization, number of electrons, and disorder on the ground-state and thermal properties of strongly-correlated electron nanoclusters. For the ordered systems, the calculations reveal for the first time that Δ tunes the interplay between the *local* Kondo and *non local* RKKY interactions, giving rise to a "Doniach phase diagram" for the nanocluster with regions of prevailing Kondo or RKKY correlations. The interplay of Δ and disorder gives rise to a Δ versus concentration $T = 0$ phase diagram very rich in structure. The parity of the total number of electrons alters the competition between the Kondo and RKKY correlations. The local Kondo temperatures, T_K, and RKKY interactions depend strongly on the local environment and are overall *enhanced* by disorder, in contrast to the hypothesis of "Kondo disorder" single-impurity models. This interplay may be relevant to experimental realizations of small rings or quantum dots with tunable magnetic properties.

I. INTRODUCTION

Magnetic impurities in non-magnetic hosts have been one of the central subjects in the physics of strongly correlated systems for the past four decades[1]. Such enduring, ongoing research effort is motivated by a constant shift and increase of scientific interest over the years, from dilute[2] to concentrated impurities[3], from periodic[4] to disordered samples[5,6], and from macroscopic[7] to nanoscale phenomena[8]. Macroscopic strongly correlated electron systems at low temperatures and as a function of magnetic field, pressure, or alloying show a wide range of interesting phenomena, such as non-Fermi-liquid behavior, antiferromagnetism, ferromagnetism, enhanced paramagnetism, Kondo insulators, quantum criticality or superconductivity[1,7]. These phenomena are believed to arise through the interplay of the Kondo effect, the electronic structure and intersite correlations. In the simplest single-impurity case, the Kondo problem describes the antiferromagnetic interaction, J, between the impurity spin and the free electron spins giving rise to an anomalous scattering at the Fermi energy, leading to a large impurity contribution to the resistivity[1]. The low-energy transport and the thermodynamic properties scale with a single characteristic energy, the Kondo temperature, $T_K \propto exp(-1/\rho(E_F)J)$, where $\rho(E_F)$ is the density of states of the conduction electrons at the Fermi energy[1]. At $T >> T_K$, the impurity spin is essentially free and the problem can be treated perturbatively. At $T << T_K$, the impurity spin is screened forming a singlet complex with the conduction electrons, giving rise to a local Fermi liquid state.

For dense Kondo or heavy fermion compounds containing a periodic array of magnetic ions interacting with the sea of conduction electrons, the physics is determined from the competition between the *non local* Ruderman-Kittel-Kasuya-Yosida (RKKY) interactions and the *local* Kondo interactions[9]. The RKKY interaction is an indirect magnetic interaction between localized moments mediated by the polarized conduction electrons, with an energy scale of order $J_{RKKY} \propto J^2\rho(E_F)$, which promotes long- or short-range magnetic ordering. On the other hand, the Kondo effect favors the formation of singlets resulting in a non-magnetic ground state. In the high temperature regime the localized moments and the conduction electrons retain their identities and interact weakly with each other. At low-temperatures, the moments order magnetically if the RKKY interaction is much larger than the Kondo energy, while in the reverse case, the system forms a heavy Fermi liquid of quasiparticles which are composites of local moment spins bound to the conduction electrons[7,9]. Thus, the overall physics can be described by the well-known "Doniach phase diagram", originally derived for the simple Kondo necklace model[10]. The description of the low-temperature state, when both the RKKY and the Kondo interactions are of comparable magnitude, is an intriguing question that remains poorly understood and is the subject of active research[9].

The interplay of disorder and strong correlations has been a subject of intensive and sustained research, in view of the non-Fermi-liquid (NFL) behavior in the vicinity of a quantum critical point[11]. Various disorder-driven models have been proposed to explain the experimentally observed[7] NFL behavior at low temperatures[5,6,7,12]. The phenomenological "Kondo disorder" approaches[5,13], based on single-impurity models, assume a distribution of Kondo temperatures caused by a distribution of either $f - c$ orbital hybridization or of impurity energy levels. These models rely on the presence of certain sites with very low T_K spins leading to a NFL behavior at low T. An open issue in such single-site Kondo approaches, is whether the inclusion of RKKY interactions would renormalize and eliminate the low-T_K spins[4,14,15,16]. An alternative view is the formation of large but finite magnetic

clusters (Griffith phases) within the disordered phase through the competition between the RKKY and Kondo interactions[6,17].

On the other hand, the possibility of making experiments in extremely small samples has lead to a resurgence of both experimental and theoretical interest of the physics of the interaction of magnetic impurities in nanoscopic and mesoscopic non-magnetic metallic systems. A few examples include quantum dots[18], quantum boxes[19] and quantum corrals[20]. Recent scanning tunneling microscope(STM) experiments[21] studied the interaction of magnetic impurities with the electrons of a single-walled nanotube confined in one dimension. Interestingly, in addition to the bulk Kondo resonance new sub peaks were found in shortened carbon nanotubes, separated by about the average energy spacing, Δ, in the nanotube. The relevance of small strongly correlated systems to quantum computation requires understanding how the infinite-size properties become modified at the nanoscale, due to the finite energy spacing Δ in the conduction band which depends on the size of the particle[8,19,22,23,24]. For such small systems, controlling T_K upon varying Δ is acquiring increasing importance since it allows to tune the cluster magnetic behavior and to encode quantum information. While the effect of Δ on the single-impurity Anderson or Kondo model has received considerable theoretical[8,19,22,23,24] and experimental[21] attention recently, its role on *dense* impurity clusters remains an unexplored area thus far. The low-temperature behavior of a nanosized heavy-electron system was recently studied within the mean-field approximation[25]. A central question is what is the effect of Δ on the interplay between the Kondo effect and the RKKY interaction

In this work we present exact diagonalization calculations for d- or f-electron nanoclusters to study the effects of energy spacing, parity of number of electrons, and hybridization on the interplay between Kondo and RKKY interactions in both *ordered* and *disordered* strongly correlated electron nanoclusters. While the properties of the system depend on their geometry and size[26], the present calculations treat exactly the Kondo and RKKY interactions, the disorder averages, and they provide a distribution of local T_K's renormalized by the intersite f-f interactions. Our results show that: i) tuning Δ and the parity of the total number of electrons can drive the nanocluster from the Kondo to the RKKY regime, i.e. a zero- temperature energy spacing versus hybridization phase diagram; ii) the temperature versus hybridization "Doniach" phase diagram for nanoclusters depends on the energy spacing ; iii) changing the total number of electrons from even to odd results in an enhancement (suppression) of the local Kondo (RKKY) spin correlation functions; iv) the Δ versus alloy concentration $T = 0$ phase diagram exhibits regions with prevailing Kondo or RKKY correlations alternating with domains of ferromagnetic (FM) order; and v) the local T_K's and the nearest-neighbor (n.n) RKKY interactions depend strongly on the local environment and are overall *enhanced* by disorder. The disorder-induced enhancement of T_K in the clusters is in contrast to the hypothesis of "Kondo disorder" models for extended systems.

The rest of the paper is organized as follows. In Sec. II, we describe the model for both the periodic and disordered clusters. In Secs. IIIA and IIIB we present results for the ground-state and thermal properties of the ordered and disordered nanoclusters, respectively. Section IV contains concluding remarks.

II. METHODOLOGY

The one dimensional Anderson lattice model is

$$H = -t\sum_{i\sigma}(c^{\dagger}_{i\sigma}c_{i+1\sigma} + H.c) + E_f\sum_{i\sigma} n^f_{i\sigma} + U\sum_i n^f_{i\uparrow}n^f_{i\downarrow} + V\sum_{i\sigma}(f^{\dagger}_{i\sigma}c_{i\sigma} + H.c.). \quad (1)$$

Here, t is the nearest-neighbor hopping matrix element for the conduction electrons, $c^{+}_{i,\sigma}(c_{i,\sigma})$ and $f^{+}_{i,\sigma}(f_{i,\sigma})$ create (annihilate) Wannier electrons in c- and f- like orbital on site i with spin σ, respectively; E_f is the energy level of the bare localized orbital, V is the on-site hybridization matrix element between the local f orbital and the conduction band and U is the on-site Coulomb repulsion of the f electrons. We use a simple nearest-neighbor tight-binding model for the conduction band dispersion, $\epsilon_k = -2tcosk$. We consider the half-filled ($N_{el} = 2N$) symmetric ($E_f = -\frac{U}{2}$) case, with $U = 5(6)$ for the periodic (disorder) case. We investigate one-dimensional rings of $N = 4$ and 6. Most of the results presented are for the $N = 6$ case, except for the results for $T > 0$ where we have used $N = 4$ sites. The exact diagonalization calculations employ periodic boundary conditions.

A. Ordered Clusters

We have investigated the ground-state properties as a function of the hybridization and the energy spacing in the conduction band, $\Delta = 4t/(N-1) = \frac{4t}{5}$. We have calculated the average $f-$ and $c-$local moments, $<(\mu^f_i)^2> \equiv < S^{f,z}_i S^{f,z}_i >$ and $<(\mu^c_i)^2> \equiv < S^{c,z}_i S^{c,z}_i >$, respectively. Here, S^f_i and S^c_i are given by

$$S^f_i = \frac{1}{2}\sum_{\sigma,\sigma'}\tau_{\sigma\sigma'} f^{+}_{i\sigma} f_{i\sigma'} \quad (2)$$

and

$$S^c_i = \frac{1}{2}\sum_{\sigma,\sigma'}\tau_{\sigma\sigma'} c^{+}_{i\sigma} c_{i\sigma'}\,, \quad (3)$$

where τ are the Pauli matrices.

We have also calculated the zero-temperature *f*-*f* and *f*-*c* spin correlation functions (SCF) $< S_i^f S_{i+1}^f > \equiv < g|S_i^{f,z} S_{i+1}^{f,z}|g >$ and $< S_i^f S_i^c > \equiv < g|S_i^{f,z} S_i^{c,z}|g >$, respectively. Here, $|g>$ is the many-body ground state and $S_i^{f,z}$ is the z-component of the f-spin at site i. As expected, the cluster has a singlet ground state ($S_g = 0$ where S_g is the ground-state spin) at half filling. We compare the onsite Kondo correlation function $< S_i^f S_i^c >$ and the nearest-neighbor RKKY correlation function $< S_i^f S_{i+1}^f >$ to assign a state to the Kondo or RKKY regimes, in analogy with mean field treatments[27]. The spin structure factor related to the equal-time $f-f$ spin correlation functions in the ground state is

$$S^{ff}(q) = \frac{1}{N} \sum_{i,j} < g|\mathbf{S}_i^f \cdot \mathbf{S}_j^f|g > e^{iq(x_i - x_j)}. \quad (4)$$

The temperature-dependent local f-spin susceptibility, $\chi^f(T)$,is

$$\frac{k_B T \chi^f(T)}{(g\mu_B)^2} = \frac{1}{Q} \sum_\alpha e^{-\frac{E_\alpha}{k_B T}} < \alpha|S^f(i) S^{Tot}|\alpha >, \quad (5)$$

where

$$Q = \sum_\alpha e^{-\frac{E_\alpha}{k_B T}} \quad (6)$$

is the partition function. Here, S^{Tot} is the z-projection of the total spin (both the *f*- and *c*-contributions), and $|\alpha>$ and E_α are the exact many-body eigenstates and eigenvalues, respectively. When $V = 0$, the localized spins and conduction electrons are decoupled and $\chi^f(T)$ is simply the sum of the Curie term due to the free f spins and the Pauli term of the free conduction electrons. For finite V, $\chi^f(T)$ decreases with temperature at low-temperatures. The specific heat is calculated from the second derivative of the free energy F, $C_v = -T\frac{\partial^2 F}{\partial T^2}$. At $V = 0$, the specific heat of the system is given by the sum of the delta function at $T = 0$ that originates from the free localized spins and the specific heat of free conduction electrons. For finite V the specific heat exhibits a double-peak structure: the high-temperature peak is almost independent of the hybridization and arises from the free conduction electron contribution, whereas the low-temperature peak varies strongly with hybridization.

B. Disordered Clusters

We consider a random binary alloy cluster, $A_{N-x}B_x$, of N=6 sites and different number of B atoms, x = 0-N, arranged in a ring described by the half-filled ($N_{el} = 2N = 12$) two-band lattice Anderson Hamiltonian in Eq.(1). We introduce binary disorder in the *f*-orbital energy ϵ_f^i ($= \epsilon_f^A$ or ϵ_f^B) and in the intra-atomic Coulomb energy U_i ($= U^A$ or U^B), to model a Kondo-type A atom with $\epsilon_f^A = -U^A/2$= -3 (symmetric case) and a mixed-valent (MV) type B atom with ϵ_f^B = -2 and $U^B = 1$. For both types of atoms $V^A = V^B = V = 0.25$. For $t = 1$, this choice of parameters leads to a degeneracy between the doubly-degenerate *c*-energy levels, $\epsilon_k = -t$, and the energy level $\epsilon_f^B + U^B$. Upon filling the single particle energy levels for any x, $N-x$ (x) electrons fill the ϵ_f^A (ϵ_f^B) levels, and two electrons the -2t conduction energy level, with the remaining $N-2$ electrons accommodated in the x+4 degenerate states at $-t$. This in turn results in strong charge fluctuations.

The temperature-dependent *f* susceptibility, $\chi_x^f(T)$, at concentration x, is given by

$$\frac{k_B T \chi_x^f(T)}{(g\mu_B)^2} = \frac{1}{Q} \sum_{C_x, \alpha_{C_x}} e^{-\frac{E_{\alpha_{C_x}}}{k_B T}} < \alpha_{C_x}|S^f(i) S^{Tot}|\alpha_{C_x} >, (7)$$

where C_x denote the configurations at concentration x, $|\alpha_{C_x}>$ and E_{C_x} are the configuration-dependent exact many-body eigenstates and eigenvalues, respectively, and Q denotes the partition function.

III. RESULTS AND DISCUSSION

A. Ordered Clusters

1. Ground State Properties

In Fig. 1 we present the variation of the local Kondo SCF $< S_i^f S_i^c >$ (squares) and the nearest-neighbor RKKY SCF $< S_i^f S_{i+1}^f >$ (circles) as a function of hybridization for two values of the hopping matrix element $t = 0.2$ (closed symbols) and $t = 1.2$ (open symbols), respectively. As expected, for weak hybridization V the local nearest-neighbor RKKY (Kondo) SCF is large (small), indicating strong short-range antiferromagnetic coupling between the $f-f$ local moments, which leads to long range magnetic ordering for extended systems. As V increases, $< S_i^f S_{i+1}^f >$ decreases whereas the $< S_i^f S_i^c >$ increases (in absolute value) saturating at large values of V. This gives rise to the condensation of independent local Kondo singlets at low temperatures, i.e., a disordered spin liquid phase. For large V the physics are *local*. Interestingly, as t or Δ decreases the *f*-*c* spin correlation function is dramatically enhanced while the *f*-*f* correlation function becomes weaker, indicating a transition from the RKKY to the Kondo regime. In Fig. 2 we present the average local *f*- (circles) and *c*- (squares) moments as a function of hybridization for two values of the hopping matrix element $t = 0.2$ (closed symbols) and $t = 1.2$ (open symbols), respectively. In the weak hybridization limit, the large on-site Coulomb repulsion reduces the double occupancy of the f level and a well-defined local f moment is formed $\langle \mu_f^2 \rangle = 1.0$ while $\langle \mu_c^2 \rangle = 0.5$. With increasing V both charge- and spin- f1uctuations become

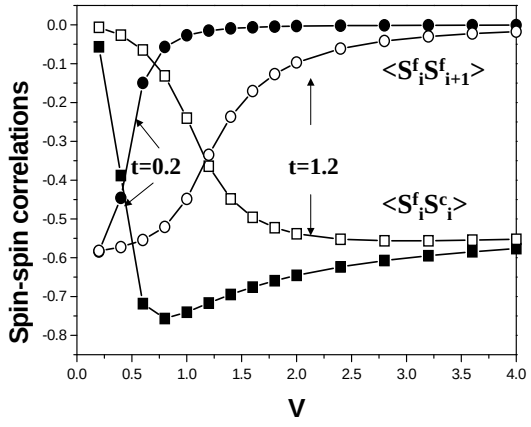


FIG. 1: Nearest neighbor f-f spin-spin correlations (circles) and on-site f-c spin-spin correlations (squares) as a function of V for two values of the hopping parameter of $t = 0.2$ (closed symbols) and $t = 1.2$ (open symbols), respectively.

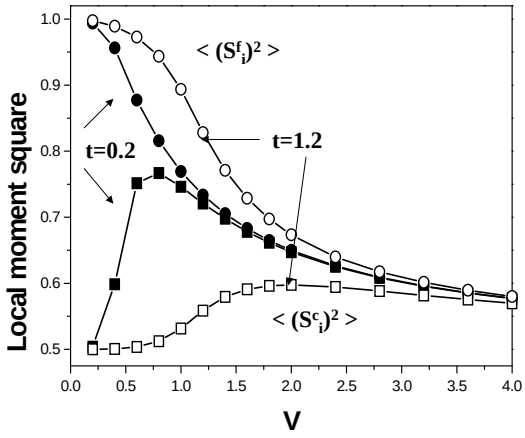


FIG. 2: f- (circles) and $c-$ (squares) local moment versus hybridization for two values of the hopping parameter of t=0.2 (closed symbols) and t=1.2 (open symbols), respectively.

enhanced and the local $f-$ moment decreases monotonically whereas the $c-$ local moment exhibits a maximum. In the large V limit both the $f-$ and $c-$ local moments show similar dependence on V, with $< \mu_c^2 > \approx < \mu_f^2 >$, indicating that the *total* local moment μ vanishes. The effect of lowering the energy spacing Δ is to decrease (increase) the $f-$ ($c-$) local moment, thus tuning the magnetic behavior of the system. Note that the maximum value of the $c-$ local moment increases as Δ decreases. This is due to the fact that for smaller t values the kinetic energy of conduction electrons is lowered, allowing conduction electrons to be captured by f electrons to screen the local f moment, thus leading to an enhancement of the local $c-$ moment. In Fig. 3 we present the energy spacing versus V zero-temperature phase diagram of the nanocluster, which illustrates the interplay between Kondo and RKKY interactions. In the RKKY region $< S_i^f S_{i+1}^f >$ is larger than the $< S_i^f S_i^c >$ and the *total* local moment is non zero; in the Kondo regime $< S_i^f S_{i+1}^f >$ is smaller than the $< S_i^f S_i^c >$, the *total* local moment vanishes, and the ground state of the system is composed of independent local singlets. The solid crossover curve indicates the $V = V_c$ or $\Delta = \Delta_c$ values, where the *local* and *non local* spin correlation functions are equal, i.e., $< S_i^f S_{i+1}^f > = < S_i^f S_i^c >$. The dashed curve denotes the set of points where the on-site *total* local moment $\mu = 0$. Thus, in the intermediate regime, which will be referred to as the *free spins* regime[11], $< S_i^f S_{i+1}^f >$ is smaller than the $< S_i^f S_i^c >$, the f moment is *partially* quenched and $\mu \neq 0$. Interestingly, we find that the *free spins* regime becomes narrower as the average level spacing Δ is reduced. This result may be interpreted as a quantum critical regime (QCP) for the nanoring due to the finite energy spacing, which eventually reduces to a quantum critical point when $\Delta \to 0$. Fig. 4 shows the

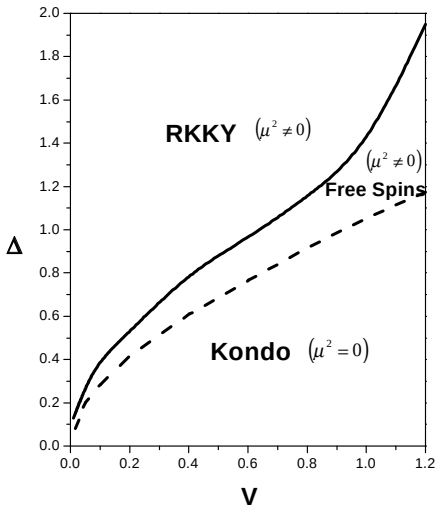


FIG. 3: Energy spacing Δ versus hybridization zero-temperature phase diagram. The solid curve denotes the crossover point of the spin-spin correlation function in Fig.1; the dashed curve denotes the set of points where the on-site total moment square $\langle(\mu_f + \mu_c)^2\rangle = 0.0 \pm 0.05$.

spin structure factor of the local f electrons $S^{ff}(q)$ for various values of V and for $t = 0.2$. As discussed earlier, the ground state of the half-filled symmetric periodic Anderson model is a singlet. For small V, the spin structure factor exhibits a maximum at $q = \pi$, indicating the presence of strong antiferromagnetic correlations between the local f moments, consistent with the large values of

$< S_i^f S_{i+1}^f >$ in Fig. 1. With increasing hybridization, the maximum of $S^{ff}(q = \pi)$ decreases and vanishes at very large hybridization, indicating that the ground state undergoes a transition from the antiferromagnetic to the nonmagnetic Fermi liquid phase. This is consistent with the zero-temperature phase diagram in Fig. 3. The spin

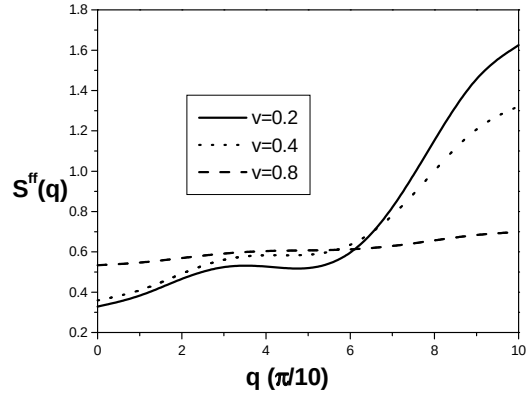


FIG. 4: Spin structure factor as a function of wave-vector for different values of V and for t=0.2.

gap as a function of hybridization V for two values of energy spacing is shown in Fig. 5. The spin gap is defined as the energy difference between the singlet ground state and the lowest-lying excited triplet ($S = 1$) state. As expected, there is a nonzero spin gap for the half-filled Anderson lattice model, which increases with hybridization. Interestingly, the spin gap dramatically increases as the average energy level spacing Δ is reduced. Thus, the energy spacing or equivalently the size of the cluster tunes the low-energy excitation energy which controls the low-temperature specific heat and susceptibility.

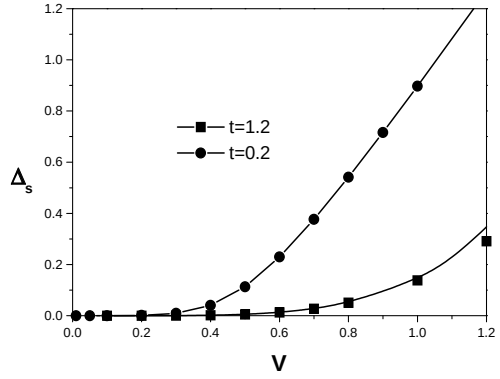


FIG. 5: Spin gap as a function of V for $t = 0.2$ and 1.2. The spin gap increases exponentially (linearly) for small (large) V.

2. Thermal Properties

The T=0 exact diagonalization results on small clusters are generally plagued by strong finite size effects[26,28]. Performing calculations at $T > 0$ gives not only the thermodynamic properties of the system, but most importantly diminishes finite-size effects for ($k_B T \gg \Delta$).

In Fig. 6, we show the nearest-neighbor f-f spin-spin correlations and on-site f-c spin-spin correlation as a function of temperature for for $t = 0.2$ and for $V = 0.2 < V_c$ and $V = 0.4 > V_c$, where $V_c = 0.25$. At high temperatures, the free moments of the f and conduction electrons are essentially decoupled. The nearest-neighbor *non local* spin correlation function falls more rapidly with T than the on-site *local* $f - c$ spin-spin correlations, indicating that the *non local* spin correlations can be destroyed easier by thermal fluctuations. For $V < V_c$, the nanocluster is dominated by RKKY (Kondo) interactions at temperatures lower (higher) than the crossover temperature, T^{cl}_{RKKY}, which denotes the temperature where the *non local* and *local* interaction become equal in the nanocluster. In the infinite system this temperature would denote the ordering Néel temperature. On the other hand, for $V > V_c$ the RKKY and Kondo spin correlation functions do not intersect at any T, and the physics become dominated by the local interactions. In Fig. 7 we present the

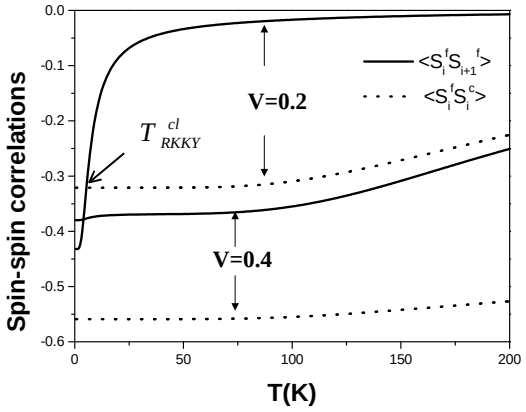


FIG. 6: Nearest-neighbor f-f and on-site f-c spin-spin correlation functions versus temperature for $t = 0.2$ and for $V = 0.2 < V_c$ and $V = 0.4 > V_c$, $V_c = 0.25$.

crossover temperature T^{cl}_{RKKY} for the cluster as a function of hybridization for different values of t. This represents the phase diagram of the strongly correlated nanocluster, which is similar to the "Doniach phase diagram" for the infinite Kondo necklace model. The phase within

the crossover curve denotes the regime where the *non local* short-range magnetic correlations are dominant. For $V < V_c$ and $T >> T^{cl}_{RKKY}$ one enters into the disordered "free" local moment regime. On the other hand, for $V > V_c$ and at low T, the nanocluster can be viewed as a condensate of singlets, typical of the Kondo spin-liquid regime. Interestingly, the T^{cl}_{RKKY} can be tuned by the energy spacing Δ or the size of the cluster. Thus, increasing Δ or decreasing the size of the nanocluster results to enhancement of the *non local* nearest-neighbor magnetic correlations and hence T^{cl}_{RKKY}. This result is the first exact "Doniach phase diagram" for a nanocluster.

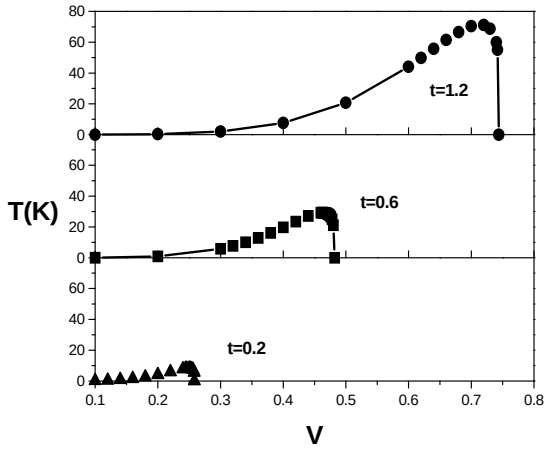


FIG. 7: Effect of energy spacing, $\Delta = \frac{4t}{N-1}$ on the exact "Doniach phase diagram" for a strongly correlated electron nanochain. The crossover curve represents the crossover temperature T^{cl}_{RKKY}, where the non local short range AF spin correlations become equal to the local on-site Kondo spin correlations.

In bulk Kondo insulators and heavy-fermion systems, the low-T susceptibility and specific heat behavior is determined by the spin gap, which for the half-filled Anderson lattice model, is determined by the ratio of V to U. On the other hand, strongly correlated nanoclusters are inherently associated with a new low-energy cutoff, namely the energy spacing Δ of the conduction electrons. Thus, a key question is how can the low-temperature physics be tuned by the interplay of the spin gap and the energy spacing. In Fig. 8 we present the local f magnetic susceptibility as a function of temperature for $t = 0.2$ and for $V = 0.2 < V_c$, $V = V_c = 0.25$, and $V = 0.4 > V_c$. For small V, the spin gap which is smaller than Δ controls the exponential activation behavior of χ^f at low T. On the other hand, in the large V limit, the spin gap becomes larger than Δ (see Fig. 5) and the low-T behavior of the susceptibility shows no exponential activation. At high T we can see an asymptotic Curie-Weiss regime, typical of localized decoupled moments. In Fig. 9, we present the specific heat as a function of temperature for $V = 0.4$

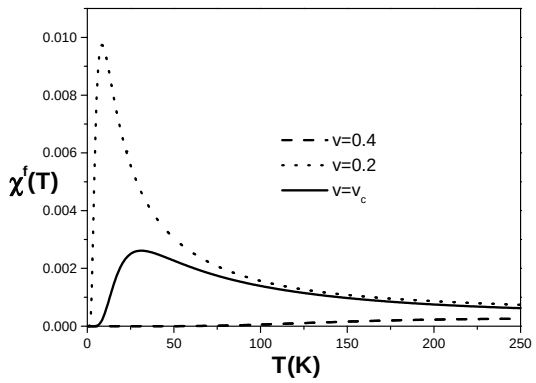


FIG. 8: Local f magnetic susceptibility as a function of temperature for $t = 0.2$ and with $V = 0.2 < V_c$, $V = V_c = 0.25$ and $V = 0.4 > V_c$.

and different t. At $V = 0$, the specific heat is given by the sum of a delta function at $T = 0$ for the localized spins and the specific heat of free fermions. As expected, by switching on the coupling V, they are combined to form a two-peak structure. The broad peak at high T is rather similar to the free-electron gas. The low-T behavior is associated with the lowest energy scale, which as in the case of the susceptibility, is determined by the lowest value between the spin gap and the energy spacing Δ. For large values of t (or Δ) the spin gap is reduced (see Fig. 5) and the spin gap is the lowest energy scale. Consequently, the low-T behavior exhibits exponential activation associated with the spin gap. On the other hand, for small energy spacing the physics become local (Kondo regime) and the low-T sharp peak shifts towards higher temperatures and becomes broader.

B. Disordered Clusters

1. Effect of Disorder

The configurations for $x \leq 3$ are shown in Fig. 10, left panel, along with the value of the spin, S_g, of the ground-state. The A (B) atoms are denoted by closed (open) circles, respectively. Except for the homogenous cases (x=0 and $x = 6$), with a $S_g = 0$ ground state, for all x there are configurations with $S_g \neq 0$. The average occupation and average LM for the periodic Kondo and MV lattices are $< n^A_f >= 1$, $< (\mu^A_f)^2 > = 0.99$, and $< n^B_f > = 1.6$, $< (\mu^B_f)^2 > = 0.43$, respectively. We carry out a detailed analysis for x=1 (S_g =2) to demonstrate the FM transition induced by a single MV atom in an otherwise Kondo cluster. Studies of extended systems have reported similar occurrence of ferromagnetism in the MV phase[29]. As expected, the singlet ground state of the $x = 0$ Kondo

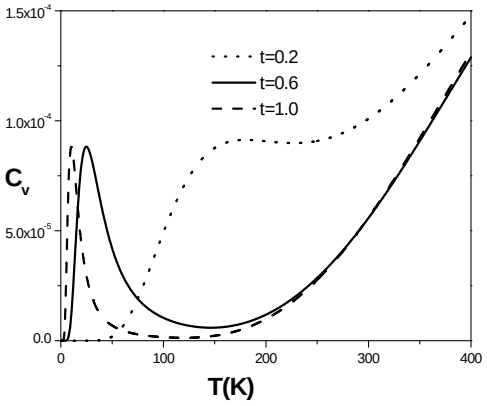


FIG. 9: Specific heat as a function of temperature with $V = 0.4$ and various values of $t = 0.2$, 0.6 and 1.0. The low-T peak for larger energy spacing is due to the spin gap.

cluster is characterized by n.n. anti-ferromagnetic (AF) *f-f* spin correlations ($< S_f^A(i)S_f^A(i+1) > =$ - 0.58). The introduction of a MV atom renders them ferromagnetic. Since U_B is small, the B impurity tends to remove charge from the the conduction band, in particular from the k-state with $\epsilon_k = -t$, which has large amplitude at the B site and at the opposite A site across the ring. Such a depletion is different for the two spin states, thus yielding a maximum value for the f-moment of the MV atom. The f-f spin correlation function between the Kondo and MV atoms are AF ($< S_f^A(i)S_f^B(i+1) > =$ - 0.23), while they are FM among the Kondo atoms ($< S_f^A(i)S_f^A(i+1) > = +0.94$). A similar result was recently found in *ab initio* calculations[30], where introducing a nitrogen impurity in small (1-5 atoms) Mn clusters induces ferromagnetism via AF coupling between the N to the Mn atoms, whilst Mn-Mn couple ferromagnetically. We find that there is a crossover in S_g from $0 \to 1 \to 2 \to 0$ (Fig. 10, right panel) indicating a reentrant nonmagnetic transition around $\epsilon_B = 2$. This almost saturated FM $S_g = 2$ domain is robust against small changes in U_B, V, ϵ_A, U_A, cluster size ($N = 7$), and band filling ($N_{el} = 10$) provided that the Kondo atom has a large LM.

In Fig. 11 we present $T\chi_x^f(T)$ as a function of temperature for different x. As $T \to 0$ (inset Fig. 11) $T\chi_x^f(T)$ approaches a finite value for $x = 1 - 4$ while it vanishes exponentially for x=0, 5 and 6. This is due to the fact that the former concentrations involve some configurations which are magnetic, while the latter have singlet ground states (Fig. 10). The stronger (weaker) low-temperature dependence for $x = 1$ ($x = 2 - 4$) is due to the smaller (larger) spin gap between the ground state and the lowest excited states. The magnetic susceptibility displays also a magnetic crossover upon varying x, and reveals a Curie-like divergence at low T for $x = 1-4$. The temperature-dependent results for the specific heat,

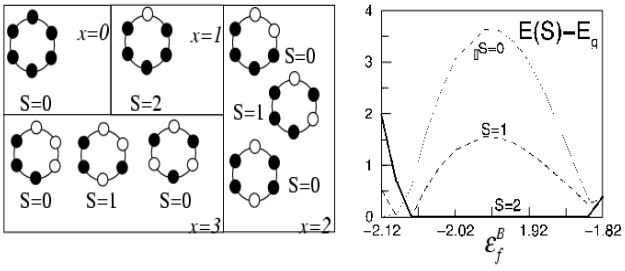


FIG. 10: Left panel: Alloy configurations for various concentrations $x \leq 3$ (the $x > 3$ cases are obtained by exchanging closed and open circles). For each $x \leq 3$ configuration, the value of the ground-state spin S_g is reported. Right panel: Energy difference (in units of $10^{-4}t$) between the lowest $S \leq 2$ eigenstates and the ground state as function of ϵ_B.

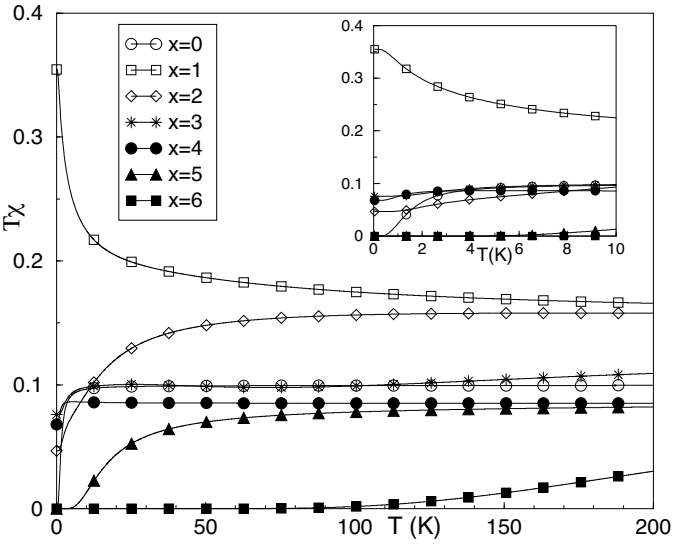


FIG. 11: Temperature dependence of the average f-susceptibility for different alloy concentrations. The inset shows the low-temperature behavior.

not reported here, show corroborative evidence of this disorder-induced magnetic crossover.

2. Effect of Energy Spacing

Next we address a number of important open issues, namely (1) the effect of Δ on the interplay between RKKY and Kondo interactions in disordered clusters, (2) the characterization of the single-impurity "Kondo correlation energy" T_K in a *dense-impurity* cluster and (3) the effect of disorder and Δ on the distribution of the local T_K's. In the following, $\epsilon_B = -2$.

In contrast with previous studies, which introduced a phenomenological distribution $P(T_K)$ of single-impurity Kondo temperatures, the advantage of the present calculations is that one calculates exactly the Kondo correlation energy: we employ the so-called "hybridization"

approach[31], with T_K defined as

$$k_B T_K(i) = E_g(V_i = 0) - E_g, \tag{8}$$

where $E_g(V_i = 0)$ is the ground-state energy of the dense-impurity cluster when V is set to zero at the i*th* site. Eq.(8) reduces to $k_B T_K = E_{band} - E_F + \epsilon_f - E_g$[22,32] in the single impurity case. Here, E_F is the highest occupied energy level in the conduction band and E_{band} is the conduction band energy. This definition of the local T_K takes into account the interaction of the f-moment at site i with the other f-moments in the system[33].

In Table I we list for the periodic, x=0, case the local Kondo *f-c* spin correlation function $< S_f^A(i) S_c^A(i) >$, the n.n. *f-f* spin correlation function $< S_f^A(i) S_f^A(i+1) >$, and the local Kondo temperature for two different values of t (The energy spacing is $\Delta = 4t/(N-1) \equiv 4t/5$). As t or Δ decreases the *f-c* spin correlation function is dramatically enhanced while the *f-f* correlation function becomes weaker, indicating a transition from the RKKY to the Kondo regime. This is also corroborated by the increase in the local $T_K(i)$. The energy spacing affects not only the magnetic (A) atoms but the MV atoms as well. Thus, increasing t drives the B atoms from the non-magnetic, NM ($n_f \approx 2$), to the MV and finally to the Kondo regime.

We next examine the role of even versus odd number of electrons on the magnetic behavior of the uniform x=0 case. For $t = 1$, changing the number of electrons from $N_{el} = 12$ to $N_{el} = 11$ results in: (a) an enhancement of the local Kondo f-c spin correlation function, $< S_f^A(i) S_c^A(i) >$ from -0.01 to -0.12; and (b) a suppression of the nearest-neighbor f-f spin correlation function $< S_f^A(i) S_f^A(i+1) >$ from -0.58 to -0.20 (Due to the broken symmetry for $N_{el} = 11$, the f-f spin correlation functions range from -0.5 to +0.02). This interesting novel tuning of the magnetic behavior can be understood as follows: For an odd-electron cluster, the topmost occupied single particle energy level is singly occupied. On the other hand, for an even-electron cluster, the topmost occupied single-particle energy level is doubly occupied, thus blocking energy-lowering spin-flip transitions. This energy penalty intrinsically weakens the Kondo correlations[19]. As expected, changing the number of electrons from even to odd changes $S_g = 0$ to $S_g = \frac{1}{2}$. For t= 0.05 (Kondo regime), the on site f-c correlation function does not depend as strongly on the parity in the number of electrons because the sites are locked into singlets. On the other hand, $< S_f^A(i) S_f^A(i+1) >$ becomes suppressed as in the case of large energy spacing. Similar results were found for the various disordered concentrations.

In Fig. 12 we present the local $T_K(i)$ as a function of the local *f-c* spin correlation function $< S_f^A(i) S_c^A(i) >$ for all Kondo (A) atoms in the singlet ground state at any concentration x for t= 0.05 and 1.0. Note the different scales both on the horizontal and vertical axis in the panels. In both panels, the closed circles correspond to the x=0 lattice case and the line is a guide to the eye.

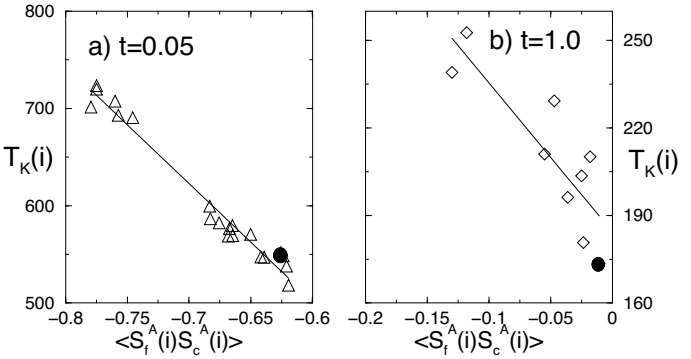


FIG. 12: A-atoms: Local Kondo Temperatures (in K) vs the local f-c spin correlation function, for different configurations and two different values of t. The closed circles refer to the $x = 0$ case and the lines are a guide to the eye.

TABLE I: Local Kondo f-c and n.n. f-f spin correlations functions and the local Kondo temperature (in K) for two values of t (in eV). The average energy spacing is $\Delta = 4t/(N-1) \equiv 4t/5$.

	$< S_f^A(i) S_c^A(i) >$	$< S_f^A(i) S_f^A(i+1) >$	$T_K(i)$
t=0.05	-0.626	-0.322	551.8
t=1.00	-0.011	-0.584	173.4

The results indicate a correlation between T_K and the *f-c* spin correlation function (the larger T_K's correspond to the more negative *f-c* values) as one would expect, since both provide a measure of the Kondo effect. For t=0.05, most of the disordered cluster configurations are in the Kondo regime ($S_g = 0$), with larger T_K values; consequently, panel (a) has a larger number of singlet configurations. The introduction of MV impurities induces a distribution of $T_K(i)$'s, whose values are overall *enhanced* compared to those for the x=0 case, except for several configurations for t=0.05, in contrast with single-site theories for extended systems[5]. It is interesting that $P(T_K)$ for t=0.05 exhibits a bimodal behavior centered about 710 and 570K, respectively: The higher T_K's originate from isolated Kondo atoms which have MV atoms as n.n. so that the local screening of the magnetic moment of the A atom is enhanced.

The effect of alloying and Δ on the RKKY versus Kondo competition for a given x is seen in Fig. 13 (left panel), where the configuration averaged local $< S_f^A(i) S_c^A(i) >_x$ and $< S_f^A(i) S_f^A(i+1) >_x$ correlation functions are plotted as a function of t. The solid curves denote the uniform x=0 case, where we drive the cluster from the RKKY to the Kondo regime as we decrease t. We find that the stronger the average Kondo correlations are the weaker the average RKKY interactions and vice versa. In the weak Kondo regime the configurations exhibit a wider distribution of RKKY interactions indicating that they are sensitive to the local environment. In contrast, in the strong Kondo regime, the Kondo (A) atoms become locked into local Kondo singlets and the

n.n
ron
lea
con

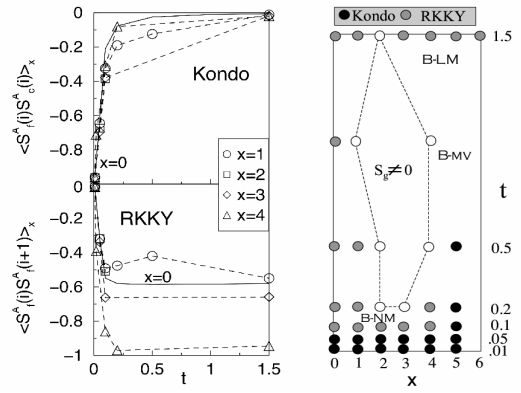


FIG. 13: Left panel: Configuration-averaged local f-c (top) and n.n. f-f spin correlations (bottom) for the A atoms as function of t. The solid line refers to the homogenous $x = 0$ case. Right panel: Zero-temperature t vs x phase diagram for the nanocluster. Black (gray) circles denote the Kondo (RKKY) regime. The white circles and the dashed contour delimit the FM region. The horizontal stripes denote the non-magnetic (NM), mixed valence (MV) and local moment (LM) behavior of the B-atoms.

Fig. 13 we present the t versus x phase diagram for the nanocluster at $T = 0$. We compare the $< S_f^A(i) S_c^A(i) >_x$ and $< S_f^A(i) S_f^A(i+1) >_x$ to assign a state of specific concentration to the Kondo or RKKY regimes (black and gray circles, respectively), in analogy with the $x = 0$ case (Table I) and with mean field treatments[27]. The horizontal gray stripes denote qualitatively ranges of t where the B atoms exhibit NM, MV and LM behavior. An interesting feature of the phase diagram is the appearance of a large FM region ($S_g \neq 0$) enclosed by the dashed line. The RKKY region at large t and large x originates from the B atoms which become magnetic. For the non FM configurations and for $x < 5$ the Kondo (RKKY) correlations of the A atoms dominate at small (large) t, in analogy with the $x = 0$ case. On the other hand, for $x = 5$ the local Kondo correlations of the single A atom at low t dominate over the *f-f* correlations between the A-B and B-B pairs. For the uniform (x=6) MV case we include only results in the large t regime, where the MV atoms acquire LM's which couple antiferromagnetically. Overall, the RKKY interactions prevail for any concentration when t is comparable or larger than the hybridization V.

IV. CONCLUSIONS

Recent advances in STM experiments have made it possible to study the electronic and magnetic properties of strongly correlated electrons in nanoscopic and mesoscopic systems. There are two main differences between nanosized clusters and the infinite lattice. First, the discrete energy levels of the conduction band states introduce a new low-energy scale, i.e., the average energy level spacing Δ. This new energy scale that competes with the spin gap can effect the low-temperature behavior of the system. Second, the results depend on the parity of the total number of electrons. If N_{tot} is odd, the ground state is doubly degenerate.

We have carried out exact diagonalization calculations which reveal that the: (1) energy spacing; (2) parity of the number of electrons; and (3) disorder, give rise to a novel tuning of the magnetic behavior of a *dense* Kondo nanocluster. This interesting and important tuning can drive the nanocluster from the Kondo to the RKKY regime, i.e. a tunable "Doniach" phase diagram in nanoclusters. We have employed the criterion of comparing the exact *non local* versus *local* spin correlation functions to determine if the nanocluster lies in the RKKY versus Kondo regime. For weak hybridization, where the spin gap is smaller than Δ, both the low-temperature local f susceptibility and specific heat exhibit an exponential activation behavior associated with the spin gap. In contrast in the large hybridization limit, Δ is smaller than the spin gap, the physics become local and the exponential activation behavior disappears. The interplay of Δ and disorder produces a rich structure zero-temperature alloy phase diagram, where regions with prevailing Kondo or RKKY correlations alternate with domains of FM order. The distribution of local T_K and RKKY interactions depends strongly on the local environment and are overall *enhanced* by disorder, in contrast to the hypothesis of single-impurity based "Kondo disorder" models for extended systems. We believe that the conclusions of our calculations should be relevant to experimental realizations of small clusters and quantum dots. For example, the recent experiments[21] of magnetic clusters on single-walled carbon nanotubes of varying size provide much flexibility for investigating the interplay of Kondo and RKKY effects at different energy scales.

Acknowledgments

The research at California State University Northridge was supported through NSF under Grant Nos. DMR-0097187, NASA under grant No. NCC5-513, and the Keck and Parsons Foundations grants. The calculations were performed on the the CSUN Massively Parallel Computer Platform supported through NSF under Grand No. DMR-0011656. We acknowledge useful discussions with P. Fulde, P. Schlottmann, P. Riseborough, A.H. Castro Neto, P.Cornaglia and C. Balseiro.

* E-mail me at: yan.luo@csun.edu.

[1] A.C.Hewson,*The Kondo Problem to Heavy Fermions*, Cambridge Press, New York, 1993.

[2] P.W.Anderson, Phys.Rev. **124** ,41 (1961); J.Kondo, Progr. Theor. Phys. **32** , 37 (1964).

[3] C.D.Bredl, S.Horn, F.Steglich, B.Luthi and R.M.Martin, Phys. Rev. Lett. **52**, 1982 (1984).

[4] H.Tsunetsugu, M. Sigrist and K.Ueda, Rev.Mod.Phys. **69** , 809 (1997).

[5] E.Miranda, V.Dobrosavljevic and G.Kotliar, Phys. Rev. Lett. **78**, 290 (1997).

[6] A.H.Castro Neto and B.A. Jones, Phys.Rev. B **62**, 14975 (2000).

[7] G.R.Stewart, Rev. Mod. Phys. **73**, 797 (2001).

[8] P.Schlottmann, Phys. Rev. B **65**, 174407 (2002).

[9] J. Lleweilun Smith and and Q. Si, Phys. Rev. B **61**, 5184 (2003).

[10] S.Doniach, Physica B **91**, 231 (1977).

[11] A. Schröder, G. Aeppli, R. Coldea, M. Adams, O. Stockert, H.V. Löhneysen, E. Bucher, R. Ramazashvili and P. Coleman, Nature **407**, 351 (2000).

[12] P.S.Riseborough, Phys.Rev.B **45**, 13984 (1992).

[13] O.O.Bernal, D.E. Maclaughlin, H.G.Lukefahr and B.Andraka, Phys. Rev. Lett. **75**, 2023 (1995).

[14] T.M.Rice and K.Ueda, Phys. Rev. Lett. **55**, 995 (1985).

[15] N.Read, D.M.Newns, and S.Doniach, Phys. Rev. B**30**, 3841 (1984); S.Burdin, A.Georges, and D.R.Grempel, Phys. Rev. Lett. **85**, 1048 (2000).

[16] S.Capponi and F.F.Assaad, Phys. Rev. B **63**,155114 (2001).

[17] E.Miranda and V. Dobrosavljevic, Phys. Rev. Lett. **86** 264 (2001).

[18] D.G.Gordon, H.Shtrikman, D. Mahalu, D.A. Magder, U.Meirav, and M.A.Kaster, Nature (London) **391**, 156 (1998).

[19] W.B. Thimm, J. Kroha, and J.V. Delft, Phys. Rev. Lett. **82**, 2143 (1999).

[20] H.C. Manoharan, C.P. Lutz, and D.M. Eigler, Nature (London) **403**, 512 (2000).

[21] T. Odom, J.L. Huang, C. Li Cheung, and C. M. Lieber, Science **290**, 1549 (2000) and references therein.

[22] H.Hu, G.M. Zhang and L. Yu, Phys. Rev. Lett. **86**, 5558 (2001).

[23] P.S. Cornaglia and C.A. Balseiro, Phys.Rev. B **66**,115303 (2002).

[24] P. Simon and I. Affleck, Phys.Rev.Lett **89**,206602,(2002).

[25] P. Schlottmann, Phys.Rev.B **65**, 024431 (2001).

[26] G.M.Pastor, R.Hirsch and B.Mühlschlegel, Phys.Rev.Lett. **72**, 3879 (1994).

[27] B.Coqblin, C. Lacroix, M.S. Gusmao and J.R. Iglesias, Phys.Rev. B **67**,064417(2003).

[28] K.Haule, J.Bonca and P. Prelovsek, Phys.Rev.B **61**, 2482 (2000).

[29] D.Meyer and W.Nolting, Phys.Rev.B **62**, 5657 (2000); D.Meyer, Solid State Comm. **121**, 565 (2002).

[30] B.K.Rao and P.Jena , Phys.Rev.Lett. **89**, 185504 (2002).

[31] P.Fulde, private communication, and P.Fulde, "Electron Correlations in Molecules and Solids", 3rd edition, Springer-Berlin-(1995).

[32] K.Yosida, Phys.Rev. **147**, 223 (1966).

[33] We also employed a second approach, $k_B T_K' = \mu_i B_c$, where B_c is the critical local external magnetic field necessary to break up the singlet bound state[23]. Comparative results of the methods will be presented elsewhere.